

Quantum walk of two anyons across a statistical boundary

Liam L.H. Lau^{1,*} and Shovan Dutta^{2,†}

¹*Gonville & Caius College, University of Cambridge, Trinity Street, Cambridge, CB2 1TA, United Kingdom*

²*T.C.M. Group, Cavendish Laboratory, University of Cambridge, JJ Thomson Avenue, Cambridge CB3 0HE, United Kingdom*

(Dated: July 6, 2022)

We model a quantum walk of identical particles that can change their exchange statistics by hopping across a domain wall in a 1D lattice. Such a “statistical boundary” is transparent to single particles and affects the dynamics only by swapping multiple particles arriving together. We find the Hanbury Brown-Twiss interference of two particles is dramatically altered by reflections of these bunched waves at the interface, producing strong measurable asymmetries. Depending on the phases on the two sides, a bunched wavepacket can get completely reflected or split into a superposition of a reflected wave and an antibunched wave. This leads to striking dynamics with two domain walls, where bunched waves can get trapped in between or fragment into multiple correlated single-particle wavepackets. These findings can be realized with density-dependent hopping in present-day atomic setups and open up a new paradigm of intrinsically many-body phenomena at statistical boundaries.

Introduction.—The behavior of identical quantum particles is dictated by their exchange statistics, i.e., the phase (θ) acquired by the wavefunction when two particles are exchanged [1]. Bosons, with $\theta = 0$, lead to black-body radiation and Bose-Einstein condensates, whereas fermions, with $\theta = \pi$, form neutron stars and the periodic table of elements. More exotic particles, with $0 < \theta < \pi$, can exist only in low dimensions [2–4]. These “anyons” are found as surface excitations on a fractional quantum Hall state [5] or spin liquids [6] and have been observed in recent experiments [7, 8], but they can also arise in one dimension (1D) [9]. Their fractional statistics has fueled intense research [10–12] and is the basis for topological quantum computing protocols [13, 14].

The rise of controllable atomic and photonic platforms has meant one can engineer particle statistics in experiments [15, 16]. In particular, Keilmann et al. [17] have shown anyons on a 1D lattice are equivalent to bosons with density-dependent hopping which has been realized in atomic setups [18–22]. Subsequently, Greschner and Santos [23] showed the statistics of these anyons is fully tunable by a Raman laser. Motivated by such possibilities, theories have found rich ground states [24–26] and dynamics [27–29]. In these studies, the exchange phase, set by complex hopping amplitudes, is spatially uniform. Yet, the protocol in Ref. [23] can be extended to nonuniform phases, which produces an intriguing scenario where anyons change their statistics by simply hopping across a domain wall. Here we explore new physics resulting from such a “statistical boundary” by modeling two-particle walks that can be monitored in experiments.

Two-body walks give a clean signature of the underlying statistics through the Hanbury Brown-Twiss (HBT) interference [30], which produces bunching of bosons and antibunching of fermions. Such walks have been realized

in atom traps [31–33] and photonic circuits [34–36], and have key technological applications [37–39]. HBT interference of anyons with a given statistics has also been examined [28, 35, 36, 40]. In 1D models [17], the anyons can have double occupancies even at $\theta = \pi$ to allow for exchange, so in this limit they behave as “pseudofermions” that retain some bunching behavior [28].

We consider statistical boundaries where the exchange phase is α on one side and β on the other side. Due to the HBT interference, the propagation occurs in the form of bunched and antibunched waves. We show the latter is unaffected by the interface since the particles move separately. On the other hand, for a boson-pseudofermion ($0-\pi$) interface, a bunched wave incident from the fermionic side is completely reflected, whereas one from the boson side is coherently split into a reflected bunched wave and an antibunched wave. Therefore, the long-time dynamics are very sensitive to initial conditions, changing dramatically as one crosses the boundary. We fully characterize this physics by global number asymmetries that can be measured, e.g., with a quantum gas microscope [33]. We predict further striking consequences, including a statistical well that can trap or successively fragment multiple bunched particles. These features are most prominent at weak interactions and large phase jumps at the boundary, which can both be tuned by Raman lasers [23]. Our study opens up investigations of correlated many-body dynamics at statistical domain walls.

Model.—Anyons on a 1D lattice with a given exchange phase θ are defined by the commutation relations $\hat{a}_i \hat{a}_j = e^{i\theta} \hat{a}_j \hat{a}_i$ and $\hat{a}_i \hat{a}_j^\dagger = e^{-i\theta} \hat{a}_j^\dagger \hat{a}_i$ for all $i < j$, where \hat{a}_i^\dagger creates an anyon at site i . There is some freedom in choosing the on-site statistics ($i = j$) [41]. We follow the convention in Refs. [17, 42] where this is bosonic; i.e., $[\hat{a}_i, \hat{a}_i^\dagger] = 1$, so multiple anyons can occupy the same site and exchange positions. This choice is further motivated by a Jordan-Wigner transform that maps such anyons to interacting bosons which can be studied experimentally [17].

We introduce anyons with a spatially varying exchange

* E-mail: lhll2@cam.ac.uk

† E-mail: sd843@cam.ac.uk

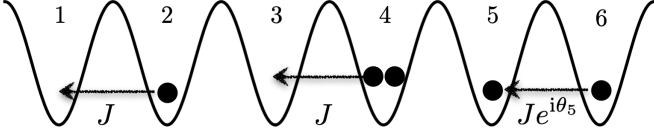


FIG. 1. Schematic of density-dependent tunneling in Eq. (4).

phase through a modified Jordan-Wigner map,

$$\hat{a}_j := e^{i \sum_{i < j} \theta_k \hat{n}_k} \hat{b}_j, \quad (1)$$

where \hat{b}_j are the boson operators and $\hat{n}_k := \hat{b}_k^\dagger \hat{b}_k = \hat{a}_k^\dagger \hat{a}_k$ is the occupation at site k . Using the relations $[\hat{b}_i, \hat{b}_j] = 0$ and $[\hat{b}_i, \hat{b}_j^\dagger] = \delta_{ij}$, we find the anyonic commutations

$$\hat{a}_i \hat{a}_j = e^{i\theta_i} \hat{a}_j \hat{a}_i \quad \text{and} \quad \hat{a}_i \hat{a}_j^\dagger = e^{-i\theta_i} \hat{a}_j^\dagger \hat{a}_i \quad (2)$$

for $i < j$; i.e., the exchange phase is set by the “left” site. This loss of reflection symmetry arises from Eq. (1) and is characteristic of anyons [10]. We are interested in cases where all exchanges are local and θ_k varies sharply across a domain wall, so particles on either side of the wall have well-defined and distinct statistics. Such an interface is “invisible” to single particles and affects the physics only by exchanging anyons between the two sides.

To probe the resulting dynamics, we adopt the Anyon-Hubbard Hamiltonian [17]

$$\hat{H} = -J \sum_j (\hat{a}_j^\dagger \hat{a}_{j+1} + \text{H.c.}) + U \sum_j \hat{n}_j (\hat{n}_j - 1)/2, \quad (3)$$

where J is the nearest-neighbor tunneling and U is an on-site interaction. Crucially, this Hamiltonian maps onto a Hubbard model for bosons via Eq. (1),

$$\hat{H} = -J \sum_j (\hat{b}_j^\dagger \hat{b}_{j+1} e^{i\theta_j \hat{n}_j} + \text{H.c.}) + \frac{U}{2} \sum_j \hat{n}_j (\hat{n}_j - 1). \quad (4)$$

Here θ_j gives an occupation-dependent Peierls phase; i.e., a hop from site $j+1$ to j yields an additional phase depending on the occupation of site j , as shown in Fig. 1. Such phases have been realized in shaken optical lattices [19–22] in a quest to simulate dynamical gauge fields [43]. Furthermore, theoretical studies have shown that Peierls phases of the specific form in Eq. (4) can be engineered by Raman-assisted tunneling [17, 23] and lattice shaking [44]. Of these, the protocol in Ref. [23] is particularly flexible and readily generalized to nonuniform θ_j by spatially modulating a Raman laser.

We study two-body walks with a statistical boundary. At any time t , the two-particle state can be expressed as

$$|\Psi(t)\rangle = \sum_j d_j(t) \hat{b}_j^{\dagger 2} |0\rangle / \sqrt{2} + \sum_{i < j} c_{i,j}(t) \hat{b}_i^\dagger \hat{b}_j^\dagger |0\rangle, \quad (5)$$

where $|0\rangle$ is the vacuum and $\sum_j |d_j|^2 + \sum_{i < j} |c_{i,j}|^2 = 1$ for normalization. Bunching or antibunching of the particles shows up in the density-density correlations $\Gamma_{i,j} :=$

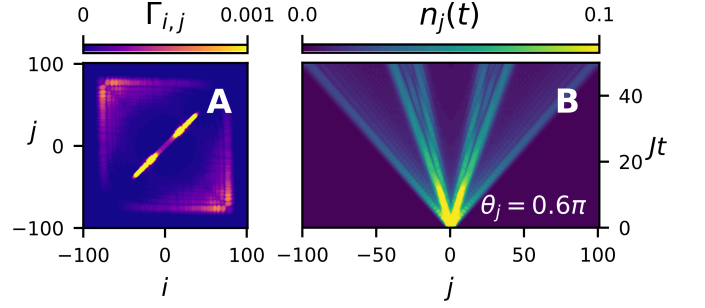


FIG. 2. Motion of two noninteracting anyons with exchange phase $\theta_j = 0.6\pi$, starting from sites $j = 0, 1$. (A) Density-density correlations $\Gamma_{i,j}$ at $Jt = 40$ and (B) density profile $n_j(t)$, showing fast antibunched and slow bunched waves.

$\langle \hat{n}_i \hat{n}_j \rangle - \delta_{ij} n_i = 2|d_j|^2 \delta_{ij} + |c_{i,j}|^2 (1 - \delta_{ij})$, and can be measured experimentally [32–36]. Here $n_i := \langle \hat{n}_i \rangle = \sum_j \Gamma_{i,j}$. We focus on neighboring initial states where the particles most strongly influence one another, as in Ref. [33]. We find the coefficients d_j and $c_{i,j}$ by exact diagonalization, using a large grid to avoid reflection from edges.

Uniform case.—Before considering a domain wall, we discuss the physics in the uniform case [28], $\theta_j = \phi$, after the particles are released from adjacent sites. For $\phi = 0$ and $U = 0$, one has pure bosons that tend to move together due to the well known HBT interference [33]. This suppresses antibunching and generates bunched waves that spread out ballistically at speed $2J$ (in units of the lattice spacing, with $\hbar = 1$). For nonzero ϕ , one finds a superposition of bunched and antibunched propagation, as shown in Fig. 2. The antibunched wave describes the two particles moving in opposite directions at speed $2J$, while the bunched wave is significantly slower. As ϕ is increased, the antibunching becomes more prominent and the bunched waves slow down further. However, even in the pseudofermion limit ($\phi = \pi$), the latter carry almost half the total weight and move at a speed $v_{\text{slow}} \approx J/5$ (see Supplement [45]). One can obtain stronger antibunching by increasing U . In the limit $U/J \rightarrow \infty$, Eq. (4) reduces to hard-core bosons that behave like free fermions [33] regardless of ϕ . Accordingly, the exchange phase is more relevant at weaker interactions.

The slow bunched wave can be explained qualitatively for $\phi \lesssim 1$ by calculating the scattering length [23], which mimics an effective repulsion

$$U_{\text{eff}} = 4J \tan^2(\phi/2) \quad (6)$$

at $U = 0$, leading to slow bound pairs [33]. However, this picture breaks down for large angles [46]. In particular, at $\phi = \pi$, $U_{\text{eff}} \rightarrow \infty$, which predicts free fermionic behavior and does not support any bunching.

Statistical boundary.—To find how the dynamics are altered by a statistical boundary, we consider a sharp domain wall such that $\theta_j = \alpha$ for $j \leq 0$ and β for $j > 0$. We focus on a boson-pseudofermion interface, i.e., $\alpha = 0$ and

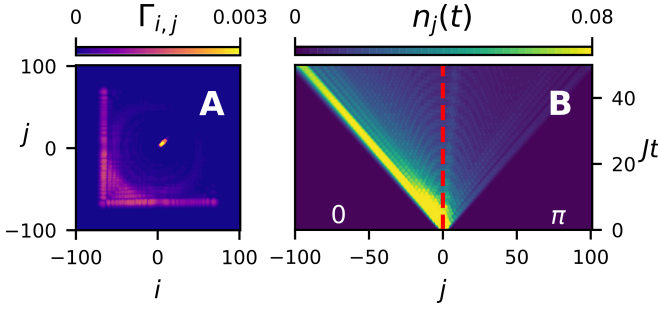


FIG. 3. Strongly asymmetric Hanbury Brown-Twiss interference of two noninteracting anyons in the presence of a boson-pseudofermion interface, $\theta_j = 0$ for $j \leq 0$ and π for $j > 0$, after they are released from sites $j = 0, 1$. (A) Two-body correlations at $Jt = 35$ and (B) density profile, showing a pronounced bunched wavefront in the bosonic side and a weak slow bunched wave in the pseudofermion side.

$\beta = \pi$, which produces the most striking departures. In a later section, we discuss how these effects fade gradually as one reduces the phase jump, increases U , or makes the interface less sharp. Note the interactions and exchange phases are both fully tunable by the protocol in Ref. [23].

Figure 3 shows what happens if the two particles are released from sites $j = 0, 1$, straddling the interface. An extremely skewed evolution ensues in which most of the weight flies off into the bosonic region as a bunched wave moving at speed $2J$. This is accompanied by some remnant antibunching. The remainder is barely visible as a weak bunched wave moving into the pseudofermion side at speed v_{slow} , carrying less than 3% of the total weight. This is in stark contrast to the symmetric walk in Fig. 2. Note the initial state can be considered “bosonic,” as the first hop does not yield any Peierls phase (see Fig. 1), so we expect a bunched wave in the boson side. One might also anticipate less transmission to the pseudofermion region due to the effective repulsion [Eq. (6)]. However, as we pointed out before, this is only a qualitative picture that misses key details. Below we show the strong asymmetry originates from a reflection of the bunched waves that is characteristic of such domain walls.

To deconstruct this effect of the interface, we consider initial states away from the junction, so that the incident waves are clearly discernible. Figure 4A shows an example where the anyons are released well inside the bosonic region at $j = -6, -5$. As in the uniform case, they start spreading out as bunched waves in both directions. When the right-moving front arrives at the interface, we find it is coherently split into two parts. One of these is reflected as a bunched wave and the other turns into antibunched motion, where one particle enters the pseudofermion side and the other goes back to the boson side. This process is sketched in Fig. 4B. Note that no bunched waves pass through the interface, which gives rise to the asymmetry in Fig. 3. The dynamics are even more striking when the

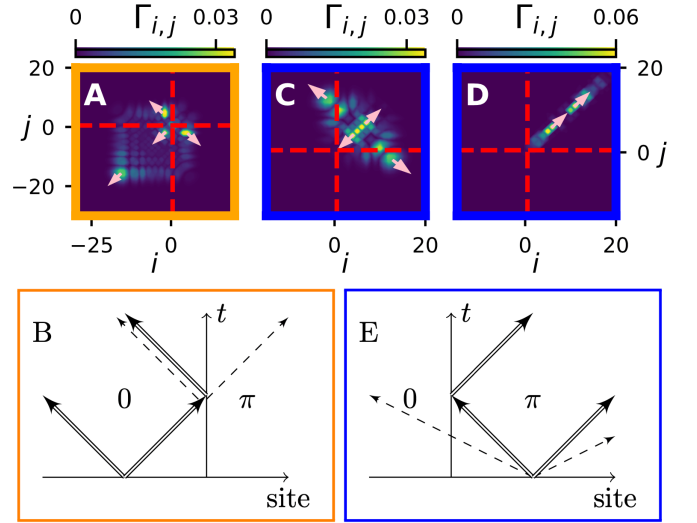


FIG. 4. Reflection of bunched waves off a $0\text{-}\pi$ statistical interface after two noninteracting anyons are released from (A, B) the boson side, $j = -6, -5$, and (C, D, E) the pseudofermion side, $j = 5, 6$. (A) Two-body correlations $\Gamma_{i,j}$ at $Jt = 5.9$, showing a bunched wave being split into a reflected bunched wave and an antibunched wave. (C) $\Gamma_{i,j}$ at $Jt = 4$, showing fast antibunched waves passing through the boundary and a slow bunched wave. (D) $\Gamma_{i,j}$ at $Jt = 47.3$, showing completely reflected slow bunched wave. (B, E) Sketch of the dynamics: double (single) arrows show bunched waves (single particles).

anyons are released in the pseudofermion side. Here one has two different timescales as in Fig. 2. There is a fast outward spreading where the anyons travel in opposite directions. Being solo, the left-moving anyon cannot see the interface and passes straight through, as in Fig. 4C. Much later, the slow bunched wave arrives and gets completely reflected, as shown in Figs. 4D and 4E.

The reflection of bunched waves incident from the boson side can be approximated by using effective hard-core interactions for $j > 0$, in accordance with Eq. (6). However, this recipe fails to capture the dynamics for pseudofermionic initial states (see Supplement [45]). The lack of transmission of the bunched waves is consistent with a large difference in group velocity between the two sides. However, we emphasize this is not single-particle physics, but a genuine consequence of exchange statistics.

The dynamics are characterized by the weights in the bunched and antibunched waves, which can be extracted from the long-time distribution. In particular, since antibunched waves contain only one particle on each side, the weight in the bunched waves moving left (right) approximately equals the probability of finding both particles in the bosonic (fermionic) side, $P_{\bullet\bullet}^{b(f)}$. These are also related to the imbalance $\mathcal{I} := (n^b - n^f)/(n^b + n^f) = P_{\bullet\bullet}^b - P_{\bullet\bullet}^f$, where $n^{b(f)}$ is the average number of particles on the boson (pseudofermion) side. As the initial positions cross the boundary, the physics changes drastically, producing sharp variations in $P_{\bullet\bullet}^{b(f)}$ and \mathcal{I} , as shown in Fig. 5. The

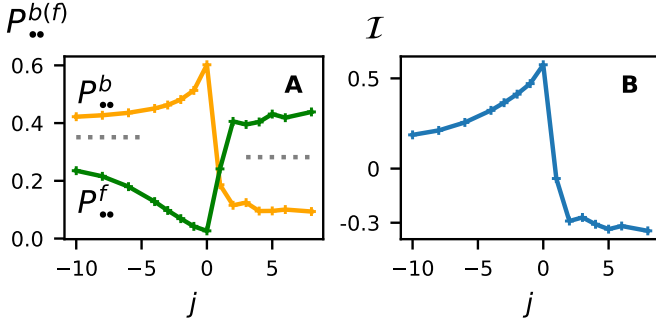


FIG. 5. Long-time asymmetries ($Jt = 100$) after the anyons are released from sites $j, j+1$, with the interface in Fig. 3. (A) Probability of finding both particles in left (orange) and right (green) halves. Dotted lines show probabilities for uniform θ_j : $P_{\bullet\bullet}^{b(f)}(0) \approx 0.35$ and $P_{\bullet\bullet}^{b(f)}(\pi) \approx 0.28$. (B) Relative number imbalance between the two halves. Abrupt changes at $j = 0$ signal very different physics on the two sides (see Fig. 4).

asymmetry falls if the release sites are far inside the boson region since the bunching is not perfect and the particles have more time to delocalize. However, we do not see this behavior on the pseudofermion side where the bunched motion is strongly bound (see Fig. 4D). Similarly, \mathcal{I} falls off with the initial separation of the particles (see Supplement [45]). Note that $P_{\bullet\bullet}^{b(f)}$ and \mathcal{I} are directly measurable in a quantum gas microscope [33].

Statistical well.—The reflections sketched in Figs. 4B and 4E lead to striking dynamics when multiple domain walls coexist. Figure 6A shows a π -0- π interface, where a bosonic region is sandwiched between two pseudofermion regions, forming a “statistical well.” Here, upon release in the middle, the particles repeatedly bounce back-and-forth as bunched waves, as per Fig. 4B. At each bounce, nearly half the incoming flux leaks out into antibunched motion, giving rise to multiple correlated single-particle waves. The reflections are more prominent for a narrow boson region which reduces delocalization. On the other

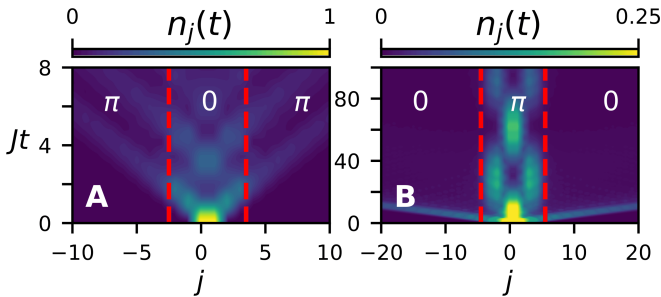


FIG. 6. Back-and-forth reflection of bunched waves inside a statistical well, following release of two noninteracting anyons at $j = 0, 1$. (A) π -0- π interface: $\theta_j = 0$ for $-2 \leq j \leq 3$. Reflections are lossy, as in Fig. 4B, producing fragmented single-particle waves. (B) 0- π -0 interface: $\theta_j = \pi$ for $-4 \leq j \leq 5$. Slow bunched waves undergo lossless reflections, and a fast antibunched wavefront flies off at short times, as in Fig. 4E.

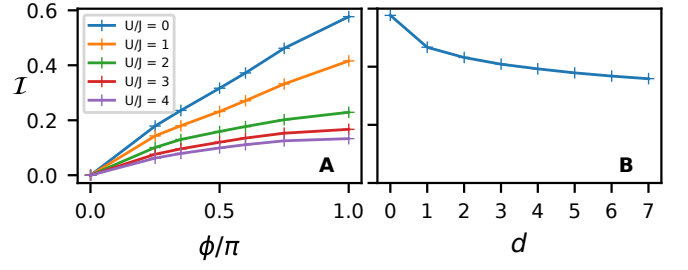


FIG. 7. (A) Long-time number imbalance between two sides of a 0 - ϕ boundary, $\theta_j = 0$ for $j \leq 0$ and ϕ for $j > 0$, with on-site interactions U , after two anyons are released from $j = 0, 1$. (B) Imbalance for a boundary of finite width d , over which θ_j grows from 0 to π , for the same initial state and $U = 0$.

hand, for a 0 - π - 0 interface, shown in Fig. 6B, the loss and delocalization are both suppressed (as in Fig. 4E), but the reflections occur on a longer timescale set by v_{slow} . Note, in both cases, the width of the surrounding region is irrelevant as the bunched waves are confined inside the well; this is confirmed by numerics (see Supplement [45]).

Experimental considerations.—So far, we have considered zero on-site interactions and maximum phase jump across a sharp interface. In Fig. 7, we show these conditions are by no means necessary for observing the physics. Figure 7A shows the imbalance \mathcal{I} between two sides of a sharp 0 - ϕ interface with $U \neq 0$, when the particles are released at the boundary (as in Fig. 3). As expected, \mathcal{I} falls monotonically as ϕ is decreased or U/J is increased. However, the change is gradual and \mathcal{I} remains large even for $U/J \sim 1$. In Fig. 7B, we consider an interface of finite width d , where θ_j varies linearly from 0 to π over d sites. Here, \mathcal{I} decreases slowly and reaches a plateau at large d , showing the physics is also not sensitive to d .

As we stated earlier, of the several protocols for engineering Anyon-Hubbard models [12, 17, 23, 44, 47], the one in Ref. [23] is most suited to our purposes. Here one uses a set of Raman lasers to control tunneling of atoms with two internal states on a tilted optical lattice. The effective U is fully tunable by a detuning. The exchange statistics is set by the relative phase of one of the lasers, which can be varied spatially to form a domain wall.

Summary and outlook.—We have investigated a novel scenario where multiple anyonic regions are separated by domain walls in the same physical system, and particles change their statistics by hopping across a wall. One can engineer this setting via occupation- and site-dependent hopping in realistic atomic setups. We have studied two-body walks that produce distinct Hanbury Brown-Twiss interference in the vicinity of such a domain wall, leading to striking consequences. In particular, the dynamics are marked by a characteristic reflection of bunched waves at the interface that is strongly asymmetric and sensitive to initial conditions. These reflections leave experimentally measurable signatures in the long-time distribution.

A distinguishing feature of such a statistical interface is that it is, by definition, transparent to single particles and affects the physics only by exchanging multiple particles arriving simultaneously. Thus, our findings strongly encourage future studies of this intrinsically many-body operation. For example, Refs. [17, 23–25, 47] have found insulating and superfluid phases of anyons as a function of their statistics, which can be combined to explore correlated transport through statistical junctions. Our work also highlights new phenomena that open up by controllable dynamical gauge fields and motivate further experimental developments at this exciting frontier [19–22, 43].

We thank Nigel Cooper for valuable feedback. SD acknowledges support from the Engineering and Physical Sciences Research Council Grant No. EP/P009565/1.

-
- [1] C. Cohen-Tannoudji, B. Diu, and F. Laloë, *Quantum Mechanics*, Vol. 2 (Wiley, London, 2006).
 - [2] J. M. Leinaas and J. Myrheim, “On the theory of identical particles,” *Il Nuovo Cimento B* **37**, 1 (1977).
 - [3] F. Wilczek, “Quantum mechanics of fractional-spin particles,” *Phys. Rev. Lett.* **49**, 957 (1982).
 - [4] G. S. Canright and S. M. Girvin, “Fractional statistics: Quantum possibilities in two dimensions,” *Science* **247**, 1197–1205 (1990).
 - [5] A. Stern, “Anyons and the quantum hall effect—a pedagogical review,” *Ann. Phys.* **323**, 204 (2008).
 - [6] H. Yao and S. A. Kivelson, “Exact chiral spin liquid with non-Abelian anyons,” *Phys. Rev. Lett.* **99**, 247203 (2007).
 - [7] H. Bartolomei et al., “Fractional statistics in anyon collisions,” *Science* **368**, 173 (2020).
 - [8] J. Nakamura, S. Liang, G. C. Gardner, and M. J. Manfra, “Direct observation of anyonic braiding statistics,” *Nat. Phys.* **16**, 931 (2020).
 - [9] F. D. M. Haldane, ““Fractional statistics” in arbitrary dimensions: A generalization of the pauli principle,” *Phys. Rev. Lett.* **67**, 937 (1991).
 - [10] F. Wilczek, *Fractional statistics and anyon superconductivity*, Vol. 5 (World scientific, 1990).
 - [11] A. Kitaev, “Anyons in an exactly solved model and beyond,” *Ann. Phys.* **321**, 2 (2006).
 - [12] S. Greschner, L. Cardarelli, and L. Santos, “Probing the exchange statistics of one-dimensional anyon models,” *Phys. Rev. A* **97**, 053605 (2018).
 - [13] C. Nayak, S. H. Simon, A. Stern, M. Freedman, and S. Das Sarma, “Non-Abelian anyons and topological quantum computation,” *Rev. Mod. Phys.* **80**, 1083 (2008).
 - [14] V. Lahtinen and J. Pachos, “A short introduction to topological quantum computation,” *SciPost Phys.* **3**, 021 (2017).
 - [15] I. M. Georgescu, S. Ashhab, and F. Nori, “Quantum simulation,” *Rev. Mod. Phys.* **86**, 153 (2014).
 - [16] E. Altman et al., “Quantum simulators: Architectures and opportunities,” [arXiv:1912.06938](https://arxiv.org/abs/1912.06938).
 - [17] T. Keilmann, S. Lanzmich, I. McCulloch, and M. Roncaglia, “Statistically induced phase transitions and anyons in 1D optical lattices,” *Nat. Commun.* **2**, 361 (2011).
 - [18] O. Jürgensen, F. Meinert, M. J. Mark, H.-C. Nägerl, and D.-S. Lühmann, “Observation of density-induced tunneling,” *Phys. Rev. Lett.* **113**, 193003 (2014).
 - [19] F. Meinert, M. J. Mark, K. Lauber, A. J. Daley, and H.-C. Nägerl, “Floquet engineering of correlated tunneling in the Bose-Hubbard model with ultracold atoms,” *Phys. Rev. Lett.* **116**, 205301 (2016).
 - [20] L. W. Clark, B. M. Anderson, L. Feng, A. Gaj, K. Levin, and C. Chin, “Observation of density-dependent gauge fields in a Bose-Einstein condensate based on micromotion control in a shaken two-dimensional lattice,” *Phys. Rev. Lett.* **121**, 030402 (2018).
 - [21] F. Görg, K. Sandholzer, J. Minguzzi, R. Desbuquois, M. Messer, and T. Esslinger, “Realization of density-dependent Peierls phases to engineer quantized gauge fields coupled to ultracold matter,” *Nat. Phys.* **15**, 1161 (2019).
 - [22] C. Schweizer, F. Grusdt, M. Berngruber, L. Barbiero, E. Demler, N. Goldman, I. Bloch, and M. Aidelsburger, “Floquet approach to \mathbb{Z}_2 lattice gauge theories with ultracold atoms in optical lattices,” *Nat. Phys.* **15**, 1168 (2019).
 - [23] S. Greschner and L. Santos, “Anyon Hubbard model in one-dimensional optical lattices,” *Phys. Rev. Lett.* **115**, 053002 (2015).
 - [24] J. Arcila-Forero, R. Franco, and J. Silva-Valencia, “Critical points of the anyon-hubbard model,” *Phys. Rev. A* **94**, 013611 (2016).
 - [25] F. Lange, S. Ejima, and H. Fehske, “Anyonic Haldane insulator in one dimension,” *Phys. Rev. Lett.* **118**, 120401 (2017).
 - [26] G. Tang, S. Eggert, and A. Pelster, “Ground-state properties of anyons in a one-dimensional lattice,” *New J. Phys.* **17**, 123016 (2015).
 - [27] Y. Hao and S. Chen, “Dynamical properties of hard-core anyons in one-dimensional optical lattices,” *Phys. Rev. A* **86**, 043631 (2012).
 - [28] L. Wang, L. Wang, and Y. Zhang, “Quantum walks of two interacting anyons in one-dimensional optical lattices,” *Phys. Rev. A* **90**, 063618 (2014).
 - [29] L. Piroli and P. Calabrese, “Exact dynamics following an interaction quench in a one-dimensional anyonic gas,” *Phys. Rev. A* **96**, 023611 (2017).
 - [30] R. Hanbury Brown and R. Q. Twiss, “Correlation between photons in two coherent beams of light,” *Nature (London)* **177**, 27 (1956).
 - [31] T. Jelts et al., “Comparison of the Hanbury Brown–Twiss effect for bosons and fermions,” *Nature (London)* **445**, 402 (2007).
 - [32] M. Schellekens, R. Hoppeler, A. Perrin, J. Viana Gomes, D. Boiron, A. Aspect, and C. I. Westbrook, “Hanbury Brown Twiss effect for ultracold quantum gases,” *Science* **310**, 648 (2005).
 - [33] P. M. Preiss, R. Ma, M. E. Tai, A. Lukin, M. Rispoli, P. Zupancic, Y. Lahini, R. Islam, and M. Greiner, “Strongly correlated quantum walks in optical lattices,” *Science* **347**, 1229 (2015).
 - [34] A. Peruzzo et al., “Quantum walks of correlated photons,” *Science* **329**, 1500 (2010).
 - [35] L. Sansoni, F. Sciarrino, G. Vallone, P. Mataloni, A. Crespi, R. Ramponi, and R. Osellame, “Two-particle bosonic-fermionic quantum walk via integrated photon-

- ics,” *Phys. Rev. Lett.* **108**, 010502 (2012).
- [36] J. C. F. Matthews, K. Poulios, J. D. A. Meinecke, A. Politi, A. Peruzzo, N. Ismail, K. Wörhoff, M. G. Thompson, and J. L. O’Brien, “Observing fermionic statistics with photons in arbitrary processes,” *Sci. Rep.* **3**, 1539 (2013).
- [37] G. Baym, “The physics of Hanbury Brown–Twiss intensity interferometry: from stars to nuclear collisions,” *Acta Phys. Polon. B* **29**, 1839 (1998).
- [38] A. M. Childs, “Universal computation by quantum walk,” *Phys. Rev. Lett.* **102**, 180501 (2009).
- [39] S. E. Venegas-Andraca, “Quantum walks: a comprehensive review,” *Quantum Inf. Process.* **11**, 1015 (2012).
- [40] G. Campagnano, O. Zilberberg, I. V. Gornyi, D. E. Feldman, A. C. Potter, and Y. Gefen, “Hanbury Brown–Twiss interference of anyons,” *Phys. Rev. Lett.* **109**, 106802 (2012).
- [41] M. D. Girardeau, “Anyon-Fermion mapping and applications to ultracold gases in tight waveguides,” *Phys. Rev. Lett.* **97**, 100402 (2006).
- [42] A. Kundu, “Exact solution of double δ function Bose gas through an interacting anyon gas,” *Phys. Rev. Lett.* **83**, 1275 (1999).
- [43] M. C. Bañuls et al., “Simulating lattice gauge theories within quantum technologies,” *Eur. Phys. J. D* **74**, 1 (2020).
- [44] C. Sträter, S. C. L. Srivastava, and A. Eckardt, “Floquet realization and signatures of one-dimensional anyons in an optical lattice,” *Phys. Rev. Lett.* **117**, 205303 (2016).
- [45] See the Supplemental Material for characterizations of the slow bunched waves, comparisons with the effective-interaction picture, dynamics of particles coincident from opposite directions with different initial separations, and effect of the width of surrounding statistical regions.
- [46] A. K. Kolezhuk, F. Heidrich-Meisner, S. Greschner, and T. Vekua, “Frustrated spin chains in strong magnetic field: Dilute two-component Bose gas regime,” *Phys. Rev. B* **85**, 064420 (2012).
- [47] L. Cardarelli, S. Greschner, and L. Santos, “Engineering interactions and anyon statistics by multicolor lattice-depth modulations,” *Phys. Rev. A* **94**, 023615 (2016).

Supplemental Material: “Quantum walk of two anyons across a statistical boundary”

SI. CHARACTERIZATION OF THE SLOW BUNCHED WAVE

In this section we investigate the effect of the exchange statistics on the speed and relative weight of the slow bunched waves discussed in the main article. As before, we consider anyons on a 1D lattice with a spatially varying exchange phase θ_j that map onto bosons with occupation- and site- dependent Peierls phase, described by the Hamiltonian

$$\hat{H} = -J \sum_j (\hat{b}_j^\dagger \hat{b}_{j+1} e^{i\theta_j \hat{n}_j} + \text{H.c.}) + \frac{U}{2} \sum_j \hat{n}_j (\hat{n}_j - 1), \quad (\text{S1})$$

where J is the tunneling, U is the interaction, \hat{b}_j^\dagger and \hat{b}_j are boson creation and annihilation operators, and $\hat{n}_j := \hat{b}_j^\dagger \hat{b}_j$. We consider noninteracting anyons ($U = 0$) in the uniform case $\theta_j = \phi$, where nonzero ϕ leads to a separation of timescales in the evolution: As shown in Fig. S1, when two particles are released from neighboring sites, the dynamics split into a fast antibunched wave, where the two anyons travel in opposite directions at speed $2J$, and a slow bunched wave, where the anyons are strongly bound and propagate more slowly.

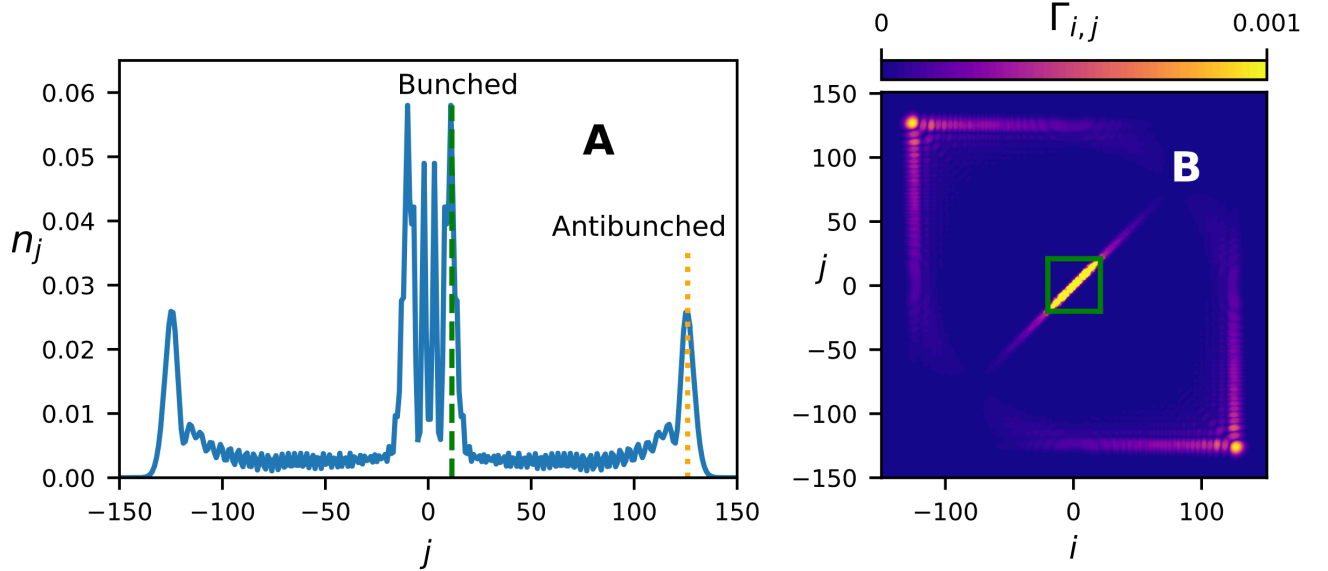


FIG. S1. Superposition of fast antibunched and slow bunched propagation with exchange phase $\theta_j = \pi$ at $Jt = 65$ after two noninteracting anyons are released from sites $j = 0, 1$. (A) Density profile showing a slow bunched mode, with sharp leading edges (dashed line), and a fast antibunched mode, peaked at $j = \pm 2Jt$ (dotted line). (B) Density-density correlations showing a clear separation between the antibunched wavefront and strongly bound bunched waves within the green square.

We use the leading edge of the bunched wave in the density profile (Fig. S1A) to characterize its speed as a function of the statistical phase ϕ . As shown in Fig. S2A, this speed falls off linearly from $v_{\text{slow}} = 2J$ at $\phi = 0$ to $v_{\text{slow}} \approx J/5$ at $\phi = \pi$. We calculate the relative weight in the bunched mode from the two-body correlations $\Gamma_{i,j} := \langle \hat{n}_i \hat{n}_j \rangle - \delta_{ij} \langle \hat{n}_j \rangle$ as $f_{\text{slow}} = \sum_{\square} \Gamma_{i,j} / 2$, where \square encloses the bunched waves (see Fig. S1B; note that $\sum_{i,j} \Gamma_{i,j} = 2$). Figure S2B shows that f_{slow} decreases monotonically with ϕ , saturating around 0.5. For comparison, we also plot the speed and weight using an effective repulsion instead of nonzero ϕ [S1], as discussed in the main text and elaborated in the next section.

SII. EFFECTIVE REPULSION

Here we provide quantitative comparisons between the exact dynamics and that generated by an effective interaction derived from the scattering length. As detailed in Ref. [S1], the low-energy collisions between two anyons with exchange

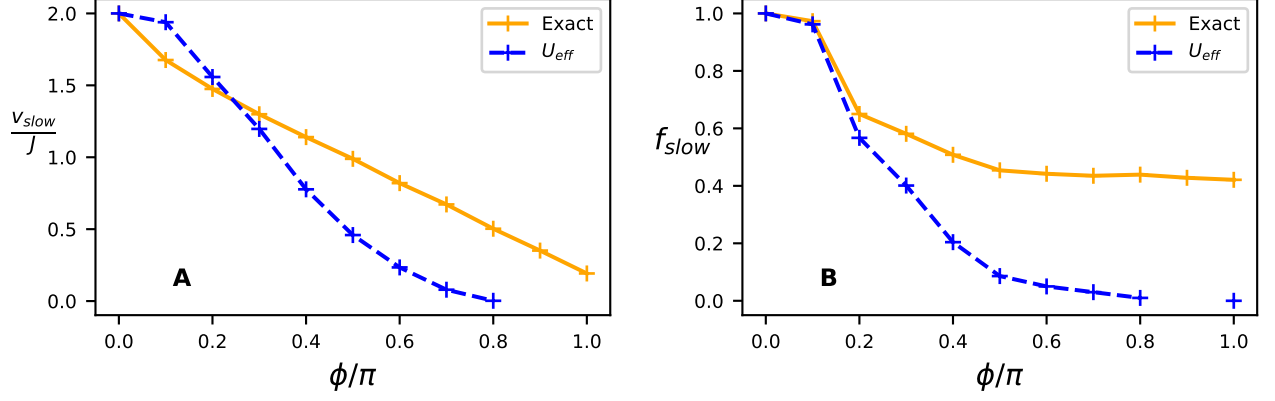


FIG. S2. (A) Propagation speed and (B) relative weight of the slow bunched waves as a function of $\theta_j = \phi$ for the exact model (solid lines) and using the effective repulsion in Eq. (S4) (dashed lines). For the latter, the bunched waves are indistinguishable from background at $\phi > 0.8$. Note the strong mismatch between the two curves at large ϕ . In particular, at $\phi = \pi$, the effective repulsion describes hard-core bosons or free fermions, so double occupancy is prohibited and bunching is not supported.

phase ϕ is characterized by the scattering length (in units of the lattice spacing)

$$a_s = \frac{-(1 + \cos \phi)}{4(1 - \cos \phi) + 2U/J}, \quad (S2)$$

which can be interpreted as originating from an effective interaction strength

$$U_{eff} = \frac{4J(1 - \cos \phi) + 2U}{(1 + \cos \phi)}. \quad (S3)$$

Note that $U_{eff}|_{\phi \rightarrow 0} = U$. In the limit $U \rightarrow 0$, we obtain an effective repulsion as a function of the exchange phase,

$$U_{eff} = 4J \tan^2(\phi/2), \quad (S4)$$

which can lead to slow-moving repulsively bound pairs [S2] through the effective Hamiltonian

$$H_{eff} = -J \sum_j (\hat{b}_j^\dagger \hat{b}_{j+1} + \text{H.c.}) + \frac{U_{eff}}{2} \sum_j \hat{n}_j (\hat{n}_j - 1). \quad (S5)$$

However, the comparisons in Fig. S2 show this effective repulsion does not capture the full dynamics when the anyons are released from adjacent sites. In particular, for angles close to π , U_{eff} diverges and does not support any bunched propagation, which is a crucial feature of the model in Eq. (S1). This breakdown is not surprising since the scattering length in Eq. (S2) becomes less than the lattice spacing (in magnitude) for $\phi \gtrsim 1$, changing its interpretation [S3].

The above discrepancy leads to very different dynamics in the vicinity of a $0-\pi$ statistical interface when the particles are released from the pseudofermionic ($\theta_j = \pi$) side, as shown in Fig. S3. For the exact model, nearly half the initial weight goes into the slow bunched mode, which is completely reflected at the boundary, as explained in the main text. On the other hand, with the effective repulsion, the particles are fully antibunched like free fermions: they travel separately in opposite directions and are not affected by the statistical boundary.

In Fig. S4, we show how the long-time asymmetries in the distribution are modified in the effective-repulsion picture for different initial positions ($j, j+1$) around a $0-\pi$ interface. As in the main text, we consider the metrics $P_{\bullet\bullet}^{b(f)}$ and \mathcal{I} , where $P_{\bullet\bullet}^{b(f)}$ is the probability of finding both particles in the bosonic (fermionic) side and $\mathcal{I} := (n^b - n^f)/(n^b + n^f)$ is the relative number imbalance between the two sides. Note the exact dynamics always produce stronger asymmetries. The agreement between the two is better when the particles are released from the bosonic side ($j \leq 0$) as the effective repulsion can approximately reproduce the reflection of the bunched waves. For $j > 0$, these are absent as in Fig. S3B, hence the imbalance \mathcal{I} is very close to zero for the effective repulsion. Note the same-side probabilities $P_{\bullet\bullet}^{b(f)}$ are still nonzero since the antibunching is not perfect and the particles are delocalized.

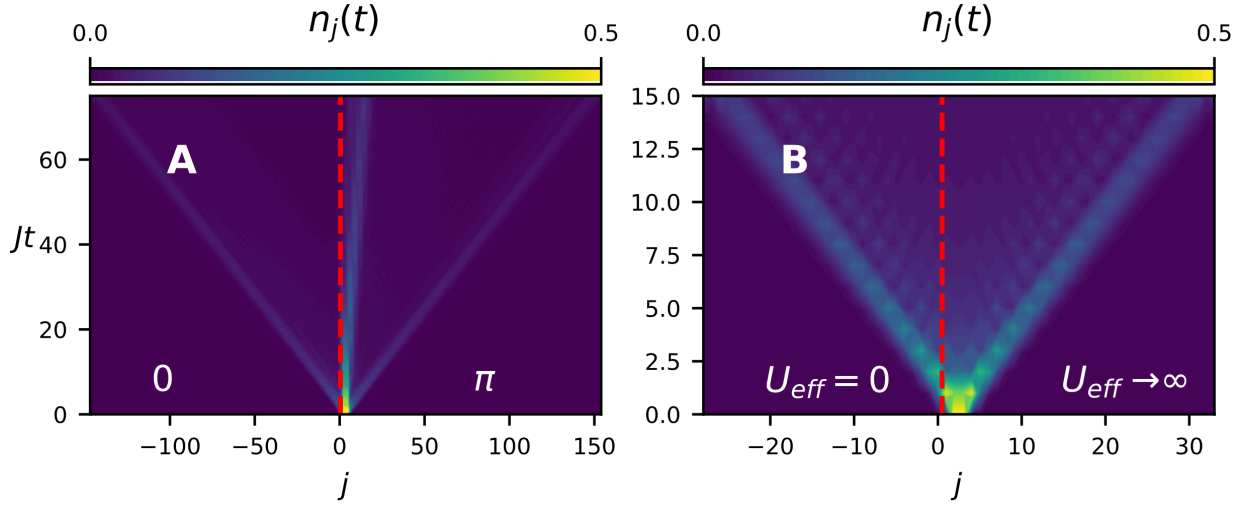


FIG. S3. Evolution of the density profile in the presence of a $0-\pi$ statistical interface ($\theta_j = \pi$ for $j > 0$), following the release of two particles from sites $j = 3, 4$ with $U = 0$. (A) Exact model [Eq. (S1)], showing a complete reflection of the slow bunched waves. (B) Using effective repulsion [Eq. (S4)], showing a fully antibunched symmetric walk that is not affected by the interface.

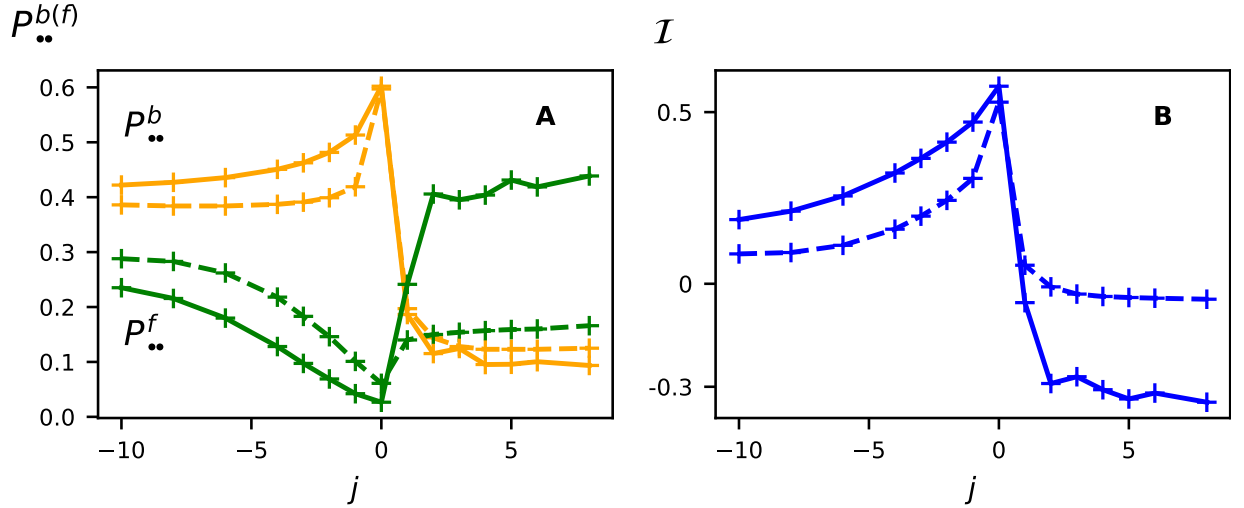


FIG. S4. Long-time asymmetries ($Jt = 100$) after the anyons are released from sites $j, j+1$ with the $0-\pi$ interface in Fig. S3 for the exact model (solid) and with corresponding effective interactions (dashed). (A) Probability of finding both particles in the left (orange) and right (green) halves. (B) Relative number imbalance between the two halves. The effective repulsion captures the qualitative features for bosonic initial states ($j \leq 0$) but produces little asymmetry for pseudofermionic initial states.

SIII. SYMMETRIC INITIAL STATES WITH LARGER SEPARATION

Here we show how the effect of a statistical boundary is reduced for larger initial distance between the two particles. As before, we focus on a $0-\pi$ interface at $j = 0$. Since it alters the dynamics only by swapping the particles, we consider symmetric initial states, where two particles are released from sites $-j+1, j$, to ensure they arrive at the boundary simultaneously from the left and the right. Figure S5A shows that the interface produces an asymmetry by sending some of this incident weight as bunched waves toward the bosonic region. As the initial separation is increased, the asymmetry falls off as shown in Figs. S5B and S5C. This is because the particles have more time to delocalize before arriving at the boundary, so less weight arrives as bunched. For large separation, the particles evolve independently and the exchange phase is redundant, so $P_{..}^{b(f)} \rightarrow (1/2)^2$. Note the separation is an odd number for the symmetric states, but we find a similar behavior even if the particles are initially separated by an even number of sites.

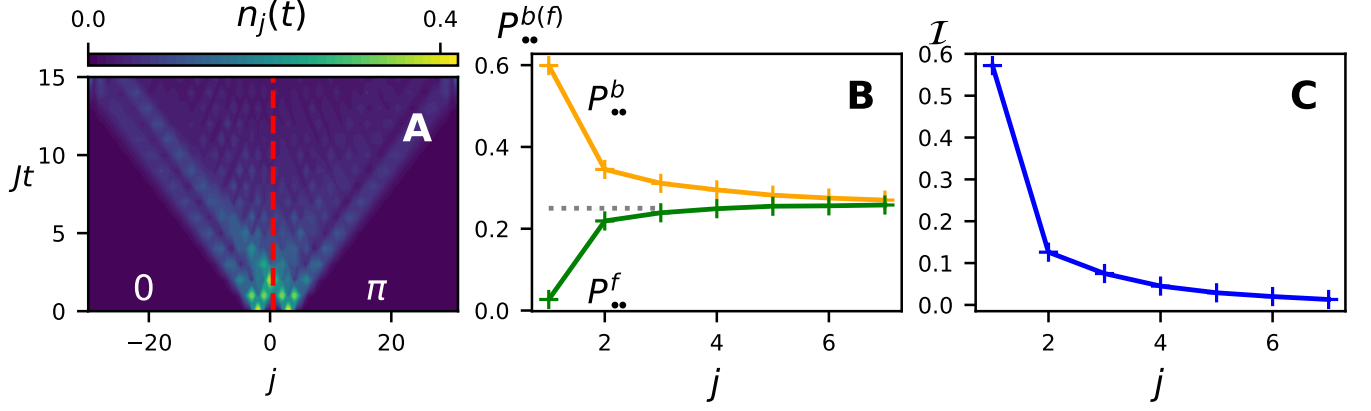


FIG. S5. Time evolution and long-time asymmetries after the anyons are released from sites $-j+1, j$ on opposite sides of a $0-\pi$ interface, with $U = 0$. (A) Density profile, showing how the interface gives rise to an asymmetry by sending bunched waves preferentially into the bosonic region. (B) Same-side probabilities $P_{..}^{b(f)}$ and (C) relative number imbalance \mathcal{I} , showing how the asymmetry falls off with larger initial separation. For $j \rightarrow \infty$, the particles move independently, so $P_{..}^{b(f)} \rightarrow 1/4$ (dotted line).

SIV. REFLECTIONS OFF A STATISTICAL REGION OF FINITE WIDTH

Consider a junction of statistical regions $\alpha-\beta-\gamma$ with exchange phases (I) $\phi_\alpha = 0, \phi_\beta = \pi, \phi_\gamma \neq \pi$ or (II) $\phi_\alpha = \pi, \phi_\beta = 0, \phi_\gamma \neq 0$, and suppose the particles are released in region α . Here we show the dynamics are insensitive to the width of region β . This is expected since no bunched waves are transmitted through the $\alpha-\beta$ interface, as sketched in Fig. 4 of the main text, which makes the $\beta-\gamma$ interface redundant. This is numerically confirmed in Fig. S6 which shows that the long-time asymmetry quickly saturates as a function of the width of region β for both (I) with $\phi_\gamma = 0$ and (II) with $\phi_\gamma = \pi$.

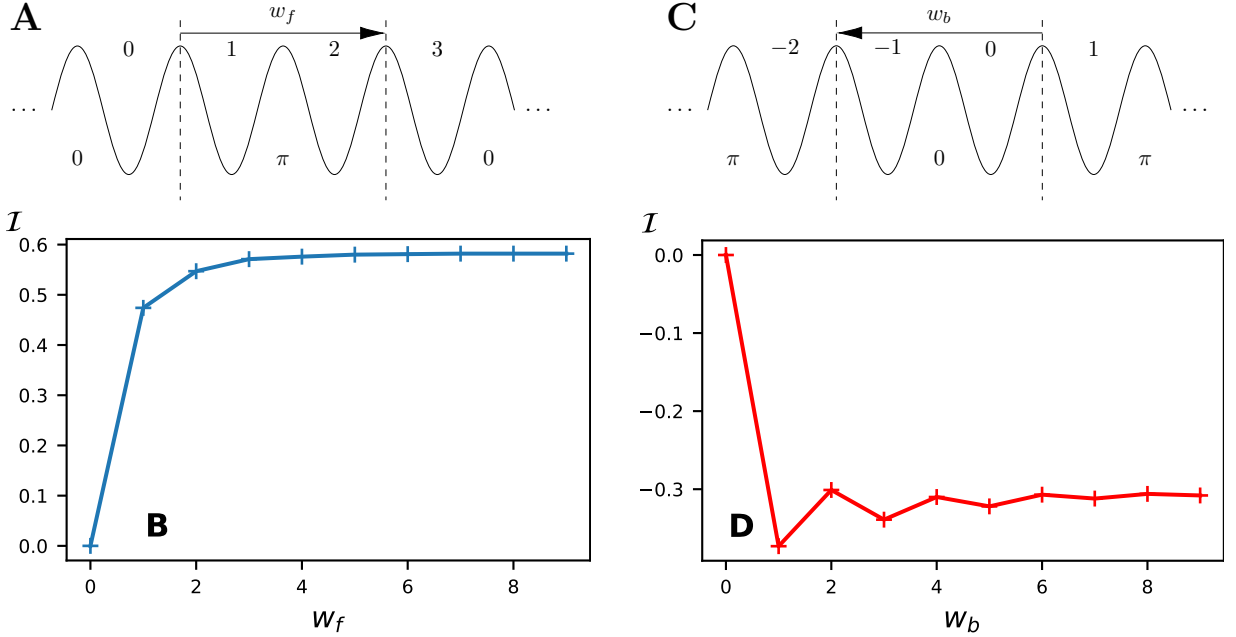


FIG. S6. Insensitivity of the dynamics of two noninteracting anyons released from one side of a statistical junction to the width of the middle region. (A) $0-\pi-0$ interface; anyons released from $j = 0, 1$, and (C) $\pi-0-\pi$ interface; anyons released from $j = 2, 3$. (B) and (D) show the corresponding number imbalance at long times ($Jt = 100$) between the regions $j \leq 0$ and $j > 0$, as in Fig. S4B. The imbalance saturates to a nonzero value as soon as the middle region spans two or more sites.

-
- [S1] S. Greschner and L. Santos, “Anyon Hubbard model in one-dimensional optical lattices,” [Phys. Rev. Lett. **115**, 053002 \(2015\)](#).
- [S2] P. M. Preiss, R. Ma, M. E. Tai, A. Lukin, M. Rispoli, P. Zupancic, Y. Lahini, R. Islam, and M. Greiner, “Strongly correlated quantum walks in optical lattices,” [Science **347**, 1229 \(2015\)](#).
- [S3] A. K. Kolezhuk, F. Heidrich-Meisner, S. Greschner, and T. Vekua, “Frustrated spin chains in strong magnetic field: Dilute two-component Bose gas regime,” [Phys. Rev. B **85**, 064420 \(2012\)](#)